

IDENTIFICATION OF THE EARTHQUAKE GROUND MOTION
AND ITS NONSTATIONARY STRUCTURAL RESPONSE
WITH THE AID OF PATTERN RECOGNITION TECHNIQUE

K. Suzuki (I)

SUMMARY

This report involves two contents and deals with an identification of nonstationary characteristics of strong earthquake motions and associated structural responses. Smoothed patterns of running power spectral density (RPSD) expressed on time- and frequency plane is introduced for the identification which is based upon the idea of pattern recognition technique. When structural response behaves nonstationarily depending on ground motion characteristics and/or time-dependent structural characteristics, another convenient method can be applied. In this method, trajectory on a complex variable number plane can quite well represent nonstationary structural response features. Some examples are demonstrated for both cases.

INTRODUCTION

There have been reported several methods of representing nonstationary time- and frequency dependent random motion characteristics. Most of them proposed in the past have intended to give nonstationary spectral representation in time- and frequency domain such as "evolutionary spectrum" (Ref. 1), "instantaneous spectrum" (Ref. 2), and "generalized spectrum" (Ref. 3).

In this report, running power spectrum density (RPSD) function $S(t, \omega)$ by Mark (Ref. 4) is utilized which can be written as

$$S(t, \omega) = 2\pi \left\langle \left| \frac{1}{2\pi} \int_{-\infty}^{\infty} x(\tau) w(t-\tau) e^{-i\omega\tau} d\tau \right|^2 \right\rangle / \int_{-\infty}^{\infty} \{w(\tau)\}^2 d\tau \quad (1)$$

where $w(\tau)$ means a kind of weighting function in time domain. Box-car type $w(\tau)$ is used here for practical simplicity. RPSD functions defined by eq.(1) can be described as two dimensional patterns taking time $t(s)$ and frequency $f(Hz)$ as the ordinate and the abscissa respectively. Spectrum computation procedure introduced here is mainly based on Akaike's algorithm (Ref. 5) which is effective for nonstationary analysis. Spectral curve shape obtained through this algorithm can usually provide us much more smoothed feature compared with that through FFT algorithm. Figure 1 (a) depicts a typical example of computed RPSD pattern for real earthquake record of ground acceleration. In this figure shade digit stands for intensive power while fainter one for weak power. The most intensive peak power value is normalized to unity and any spectral value for an arbitrary point $[t(s), f(Hz)]$ on the time- and frequency plane should be adjusted to one of ten levels classified with a logarithmic scale.

Although this RPSD pattern gives us nonstationary characteristics for a specific ground motion of an earthquake like Fig. 1(a), it still remains considerably rough feature particularly along the time domain. Therefore, an adequate filtering operation is required in order to remove these surface ruggedness. By applying the idea of the image technology, smoothed filtered

(I) Associate Professor of Mechanical Engineering, Tokyo Metropolitan University, Tokyo, Japan

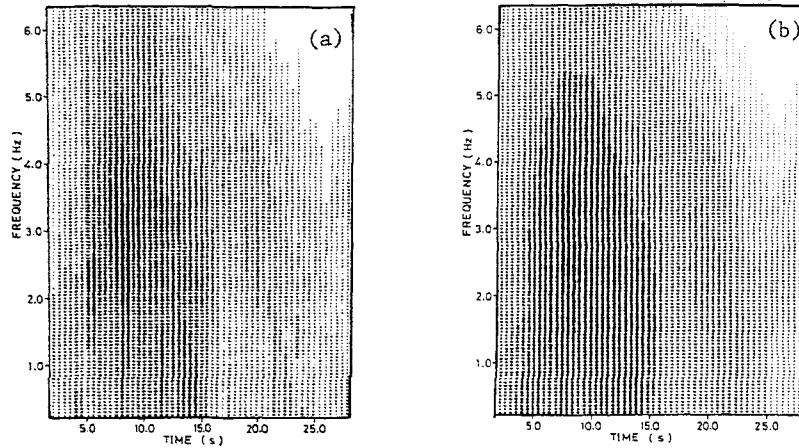


Figure 1 RPSD Pattern of Earthquake Motion [Taft N29°E] (a) and Its Smoothed Pattern (b)

pattern $s_m(t, f)$ can be formulated from the original pattern $s_o(t, f)$ with the aid of convolution integral described as

$$s_m(t, f) = \int_{\alpha} \int_{\beta} h(t - \alpha, f - \beta) s_o(t, f) d\alpha d\beta \quad (2)$$

where $h(t, f)$ is a kind of transfer function defined on (t, f) plane the form of which should be adequately selected according to the required filtering effect. Since "low-pass filtering effect" is expected in this study, transfer function could be proposed as

$$h(t, f) = h_0 \exp\left\{-\frac{(t^2 + f^2)}{2\sigma^2}\right\} \quad (3)$$

where h_0 means a constant giving smoothing effect. For convenience' sake of numerical computation, $h(t, f)$ has to be assumed to have a digitized formulation as $h(t_i, f_j)$; [$i = 1, 2, \dots, n$; $j = 1, 2, \dots, m$] where $n \times m$ means a size of matrix with respect to this digitized transfer filter. Figure 1(b) shows thus computed smoothed RPSD pattern corresponding to the original RPSD in Fig. 1(a).

IDENTIFICATION OF NONSTATIONARY EARTHQUAKE MOTIONS USING RPSD PATTERNS

Based on the RPSD pattern above introduced, any nonstationary earthquake record can be identified taking following three basic features as representative remarks;

- (1) number of dominant RPSD peaks (two peaks at most considered)
- (2) degree of RPSD's spread around dominant peaks (either in time- or frequency domain)
- (3) relative location of two peaks (if two peaks exist)

These remarks are conveniently incorporated into "peak function" described as

$$p(t, f) = g_T(t) \cdot g_F(f) \quad (4)$$

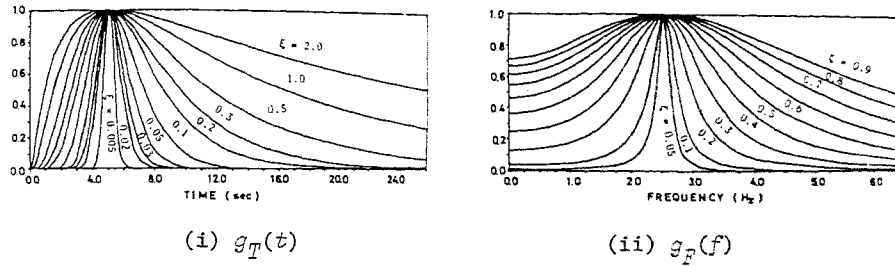


Figure 2 Examples of $g_T(t)$ and $g_F(f)$

where $g_T(t)$ means time-dependent shaping function which shows nonstationary power spectral envelope while $g_F(f)$ does power distribution along frequency domain. It was assumed in this study that $g_T(t)$ and $g_F(f)$ are given as following representation referring several previous works (Ref. 3, 6) concerning nonstationary ground motion analysis,

$$\left. \begin{aligned} g_T(t) &= \frac{1}{t} \exp\left\{-\frac{(\ln t - \mu(\xi))^2}{2\xi^2}\right\} \frac{1}{t_{\max}(\xi)} \\ g_F(f) &= \frac{1 + [2\xi\{f/f_a(\xi)\}]^2}{[1 - \{f/f_a(\xi)\}]^2 + [2\xi\{f/f_a(\xi)\}]^2} \frac{1}{f_{\max}(\xi)} \end{aligned} \right\} \quad (5)$$

In these equations ξ and ζ are taken with respect to evolutionary shape of the individual RPSD peak while $t_{\max}(\xi)$, $f_{\max}(\zeta)$ and $f_a(\zeta)$ are certain deterministic functions of ξ and ζ . Typical examples of $g_T(t)$ and $g_F(f)$ are demonstrated in Fig. 2 taking ξ and ζ as parameter. Representative values for ξ are adopted 0.03 and 0.1 and those for ζ , 0.2, 0.5 and 0.7. When two peaks have to be considered, equation (4) can be modified as

$$p_n(t, f) = \{p_1(t, f) + \beta p_2(t, f)\} \frac{1}{p_{\max}(\beta)} \quad (6)$$

by simple superposition of two function $p_1(t, f)$ and $p_2(t, f)$ where β means ratio of two representative peak intensities. Once realistic values on ξ and ζ are given and an adequate shape of peak functions considering general characteristics of actual strong ground motion is determined, a standard reference RPSD pattern can be generated artificially for the convenience of identification procedure to be followed.

Identification in the study is carried out according to the idea of the pattern image recognition technique. Concept of "complex resemblance method" which has been utilized in the field of image technology (Ref. 7) is introduced. Applying this method, correlation (resemblance) with respect to a standard RPSD pattern $Q(t, f)$ in (t, f) plane can be evaluated fairly easily by "complex resemblance function" S^* determined by

$$S^* = \frac{\sqrt{\left\{\sum_{(t,f)} \phi_0 R(t, f)\right\}^2 + \left\{\sum_{(t,f)} \phi_1 R(t, f)\right\}^2 + \left\{\sum_{(t,f)} \phi_2 R(t, f)\right\}^2}}{\|R(t, f)\|} \quad (7)$$

In this representation, ϕ_0 , ϕ_1 and ϕ_2 are obtained by using orthogonal rela-

tionship among three functions; f_0 , f_1 and f_2 as

$$\phi_0 = \frac{f_0}{\|f_0\|}, \phi_1 = \frac{f_1 + f_2}{\|f_1\| + \|f_2\|}, \phi_2 = \frac{f_1 - f_2}{\|f_1\| - \|f_2\|} \quad (8)$$

whereby θ is evaluated by

$$\theta = \frac{\sum_{(t,f)} f_1 \cdot f_2}{\|f_1\| \cdot \|f_2\|} \quad (9)$$

Functions f_0 , f_1 and f_2 themselves are calculated as

$$f_0 = Q(t, f), f_1 = \frac{\partial Q(t, f)}{\partial t}, f_2 = \frac{\partial Q(t, f)}{\partial f} \quad (10)$$

In these equations $\|f_i\|$ means the mathematical norm for functions f_i ($i = 0, 1, 2$) within (t, f) domain. Consequently, it can be said that S^* in eq. (7) physically means a space correlation function between a specific RPSD pattern $R(t, f)$ and the artificial standard pattern $Q(t, f)$. As a result, once $R(t, f)$ with respect to some actual nonstationary ground motion is calculated, identification can be easily performed with the aid of the resemblance function S^* .

Figure 6 explains schematically the idea of this pattern recognition aided identification of earthquake motions proposed in the study (Ref. 8). The author provides in this investigation representative 8 standard categories for $Q(t, f)$ half of which are for double peaks case. The results of identification for several strong earthquake accelerations recorded in U.S. and Japan according to this procedure are summarized as shown in Table 1.

Table 1 Some Results of Identification for Earthquake Motions

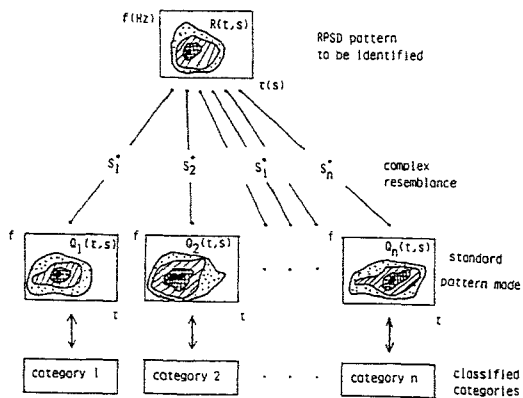


Figure 3 Schematic Conception of Pattern Recognition and Identification

Category	Peak Shape	Identified Earthquake Motions
I - a	$\xi = 0.2$ $\zeta = 0.7$	Managua NS,EW, San Fernando NS
I - b	$\xi = 0.03$ $\zeta = 0.5$	San Fernando (a) S08°W
I - c	$\xi = 0.2$ $\zeta = 0.2$	Kushiro NS, Miyagiken-oki NS, Tokachi-oki EW, Amagasaki UD, San Fernando (b) N29°E, San Fernando (c) EW, Managua UD
I - d	$\xi = 0.03$ $\zeta = 0.2$	Niigata NS,EW, Kushiro EW, San Fernando (a) S82°E, UD, San Fernando (c) UD
II - a	$\xi_1 = 0.1$ $\xi_2 = 0.7$ $\zeta_1 = 0.1$ $\zeta_2 = 0.7$	Taft S69°E, N21°E, El Centro NS,EW, El Centro (d) NS,EW,UD
II - b	$\xi_1 = 0.1$ $\xi_2 = 0.03$ $\zeta_1 = 0.5$ $\zeta_2 = 0.5$	Amagasaki Tr., San Fernando (b) S61°E, San Fernando (c) ns
II - c	$\xi_1 = 0.03$ $\xi_2 = 0.1$ $\zeta_1 = 0.5$ $\zeta_2 = 0.5$	Tokachi-oki NS, San Fernando EW
II - d	$\xi_1 = 0.1$ $\xi_2 = 0.1$ $\zeta_1 = 0.2$ $\zeta_2 = 0.5$	Niigata UD, Tokachi-oki UD, Amagasaki Lg., Kern County (e) N21°E, San Fernando (b) UD

APPLICATION FOR THE ARTIFICIAL GENERATION OF NONSTATIONARY GROUND MOTION

Once several standard RPSD patterns have been established, we can inversely generate nonstationary ground motion earthquake which should belong to a specific category corresponding to the standard RPSD pattern. Generally nonstationary earthquake motion $Y(t)$ can be expressed by

$$Y(t) = \sum_{n=1}^N X(t, f_n) \cos(2\pi f_n t + \phi_n) \quad (11)$$

where $X(t, f_n)$ is the Fourier transformed amplitude with respect to a specific discrete value for f_n and ϕ_n is a randomly distributed phase angle. It can be assumed that $X(t, f_n)$ is given by

$$X(t, f_n) = C \cdot \sqrt{Q(t, f_n)} \quad (12)$$

in which C is a constant and $Q(t, f_n)$ is an artificial standard pattern. In Fig. 4 examples of thus generated nonstationary earthquake motions which is accompanied with the corresponding RPSD are depicted for a single and double peak cases. Satisfactory good correspondence can be observed. Such a correspondence can be recognized for any other categories established in Table 1.

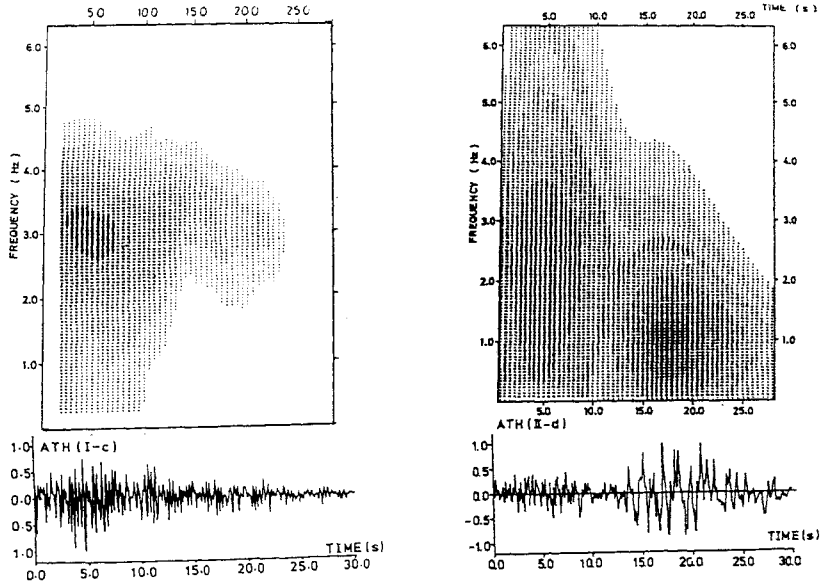


Figure 4 Standard RPSD Patterns and Corresponding Nonstationary Artificial Earthquakes for Single and Double Peaks

TRAJECTORY OF NONSTATIONARY RESPONSE CHARACTERISTICS

Let us here consider the characteristic equation of a single-degree-of-freedom damped system by using Laplacian operator s as

$$s^2 + 2\zeta\omega_0 s + \omega_0^2 = 0 \quad (13)$$

where ζ means a damping ratio and ω_0 does a natural frequency of this system. From eq. (13) characteristic roots can be derived as

$$s = -\zeta\omega_0 \pm i\sqrt{1-\zeta^2}\omega_0 \quad (14)$$

Using the time shift operator $z = \exp(s\tau)$ [τ ; time step of a nonstationary response process $x(t)$ to be analyzed], mapping relation for this transition which demonstrates relation between $s\tau$ -plane and z -plane can be shown in Fig. 5 (Ref. 9).

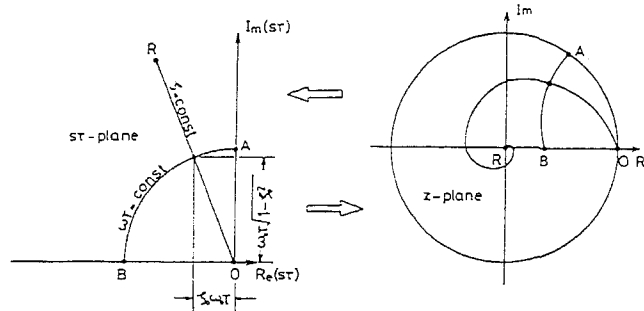


Figure 5 Mapping Correspondence between $s\tau$ -plane and z -transformed plane

It has become very convenient to apply such representation especially when we have to treat frequency- and damping variant narrow band structural response motions. Taking real part as the abscissa and imaginary part as the ordinate, point P_1 on $s\tau$ -plane in Fig. 6 which corresponds to the state at a time instant t_1 presents dominant frequency ω_1 and damping ζ_1 through the point $(-\zeta_1\omega_1\tau, \omega_1\sqrt{1-\zeta_1^2}\tau)$ in $s\tau$ -plane. If this state P_1 moves to P_2 at time t_2 as shown in the figure, trajectory P_1P_2 corresponds to nonstationary narrow band motion in which frequency and damping from (ω_1, ζ_1) to (ω_2, ζ_2) . Circular arcs A_1B_1 and A_2B_2 in Fig. 6 give constant value of ω_1 and ω_2 respectively, while straight lines OP_1 and OP_2 give the constant damping ζ_1 and ζ_2 respectively. General representation corresponding to the state (ω_i, ζ_i) at any arbitrary time instant t_i can be written as

$$\left. \begin{aligned} \omega_i &= \sqrt{[R_s(s\tau)]^2 + [I_m(s\tau)]^2} / \tau \\ \zeta_i &= -R_s(s\tau) / \omega_i \tau \end{aligned} \right\} \quad (15)$$

NUMERICAL EXAMINATIONS AND PRACTICAL APPLICATIONS

Numerical examination was performed by using the simplest nonstationary structural model, namely, the frequency variant or the damping variant model having a single-degree-of-freedom. As the frequency variant system, we take the model whose frequency decreases from 10 Hz to 2 Hz keeping damping constant. Examples of such nonstationary trajectories are shown in Fig. 7. On the other hand Fig. 8 corresponds to another nonstationary trajectories where-by damping ratio varies from 0.01 to 0.5 under constant natural frequency.

Although lines in Fig. 7 do not always coincide with those corresponding theoretical straight lines mainly because of high sensitivity of damping characteristics, distinctive nonstationary response behaviour can be achieved. In contrast with this case, trajectories for damping variant systems follow quite well theoretical ones.

As a simple example for actual application, the author shows results using some experimental data. Frequently, we can observe nonstationary response behaviour for the structural systems when they are subjected to excess dynamic loadings. For instance, piping response to excess dynamic excitations shows so-called "softening stiffness features" during excited period before the inelastic deformation and the crack initiation. Figure 9 shows a typical nonstationary trajectory for simple beam type piping model provided for the excited test under quasi-resonance condition. As a result, an initial state of $f_0 = 22.5$ Hz and $\zeta = 0.08$ changes after about 40 minutes into the state of $f_0 = 20.5$ Hz and $\zeta = 0.10$. Such an approach can develop to more general situations many of which frequently appeared in the seismic excitation problem.

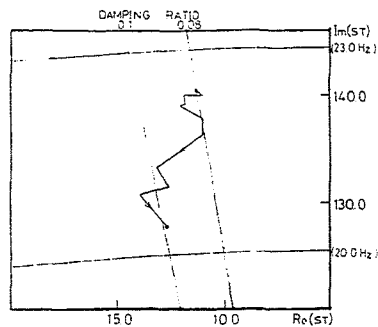


Figure 9 Trajectory of Nonstationary Piping Response under Random Excitation

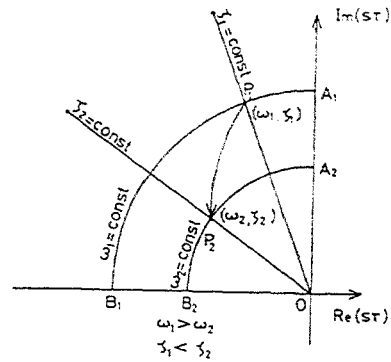


Figure 6 Trajectory of Nonstationary Moving Point

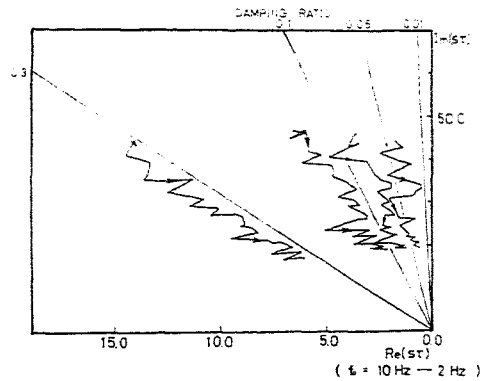


Figure 7 Trajectory of Frequency Variant Model ($f_0 = 10$ Hz to 2 Hz)

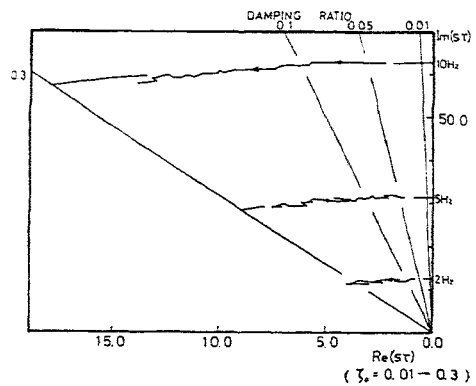


Figure 8 Trajectory of Damping Variant Model ($\zeta = 0.01$ to 0.3)

CONCLUSIONS AND ACKNOWLEDGEMENTS

The principal results obtained in this study can be summarized as follows;

- 1) Applying the idea of a pattern recognition technique, nonstationary earthquake ground motion characteristics can be identified by using RPSD patterns which are drawn on to the frequency and time plane.
- 2) The RPSD pattern for a specific earthquake motion is adequately classified based upon the artificially "categorized" standard pattern model.
- 3) Nonstationary earthquake motions which should belong to any standard category are arbitrarily generated with the aid of corresponding RPSD pattern.
- 4) Trajectory expressed in complex sT -plane is very convenient to show the nonstationary response behaviours, particularly, those having narrow band characteristics.

Finally the author would like to show his sincere thanks to Dr. N.Shimizu at Chiyoda Chemical Engineering & Construction Co. Ltd. for his valuable discussions and advices. He is also deeply grateful to Messrs. S.Aoki, S.Tozawa, A.Nakashima and Y.Temmyo who have made co-operative works in his laboratory.

REFERENCES

- 1) Priestley, M.B. (1965), "Evolutionary Spectra and Non-stationary Processes", J. Royal Statistical Society, Ser. B., No.2.
- 2) Page, Chester H. (1952), "Instantaneous Power Spectra", J. Applied Physics, Vol. 23, No.1.
- 3) Hoshiya, M.,(1975), "Spectral Analysis of Nonstationary Stochastic Process", Journal of Japanese Society of Civil Engineers, Vol.60, No.3.
- 4) Mark, W.D., (1970), "Spectral Analysis of the Convolution and Filtering of Nonstationary Stochastic Processes", J. Sound Vib., Vol.11, No.1.
- 5) Akaike, H. and Nakagawa, T., "Statistical Analysis and Control of Dynamic System", Science-sha, Tokyo, 1972.
- 6) Kameda, H., (1975), "On the Calculation Method of Nonstationary Power Spectrum for Ground Motion", Transaction of J.S.C.E., Vol.235.
- 7) Nakata, K., "Pattern Recognition and Its Applications", Korona Publication Co. Ltd., Tokyo, 1978.
- 8) Suzuki, K., Tozawa, S. and Temmyo, Y., (1982), "Identification of Strong Earthquake Ground Motion by Using Pattern Recognition Techniques for Aseismic Design", Transaction of Japanese Society of Mechanical Engineers, Vol.49, No.437.
- 9) Suzuki, K. and Nakashima, A., (1981), "Practical Damping Estimation Method by Using the Spectral Analysis Techniques Based on the Auto-Regressive Fitting Equation", Transaction of Japanese Society of Mechanical Engineers, Vol.48, No.433.